COBEM 2023 27TH INTERNATIONAL CONGRESS OF MECHANICAL ENGENEERING

ABCM Brazilian Society of Mechanical Sciences and Engineering
27th ABCM International Congress of Mechanical Engineering
December 04-08, 2023, Florianópolis-SC, Brazil

COB-2023-2046
DEVELOPMENT OF A MICROCONTROLLER FOR MANUFACTURE OF CERAMICS SCAFFOLDS BY FREEZE CASTING PROCESS

João Paulo Santiago de Assis Silva
Alysson Martins Almeida Silva
Jones Yudi Mori Alves da Silva
Adriano Possebon Rosa
Ceramic and Nanostructured Materials Laboratory (LMCNano)
Department of Mechanical Engineering, Faculty of Techonology, University of Brasilia, Brazil
santiagojp@unb.br, alyssonmartins@unb.br, jonesyudi@unb.br, aprosa@unb.br

Abstract. *This study presents the development of a microcontrolled system for the manufacture of ceramic materials with a defined pore structure. This technique, known as freeze casting, allows for the control of pore formation in different materials through the sublimation of solvent crystals solidified under cryogenic conditions. The proposed equipment uses a PID type control to maintain the temperature with a maximum variation of ±1 ºC, in the range of -196 ºC to -130 ºC. The effectiveness of the equipment was validated through the production of graphene oxide and chitosan monoliths. Characterization was done using Scanning Electron Microscopy. In which it can be verified the variation in the pore structure using different freezing temperatures.*

Keywords: *Freeze-casting, Pore Structures, Microcontroller.*

1. INTRODUCTION

Materials produced by the freeze-casting process have attracted considerable attention in many research areas and industries due to their extensive potential applications. These materials stand out for their defined pore structure, allowing for high absorption capacity, low thermal conductivity, and superior permeability (Sousa *et al.*, 2021). These versatile properties allow their application in various areas, from gas filtration (Christiansen *et al.*, 2020; Souza *et al.*, 2014) to bone tissue engineering (Scotti and Dunand, 2018; Yin and Naleway, 2022). Among the various methods to produce porous materials, freeze casting stands out for its ability to create highly organized pores. This feature has increased the popularity of the technique, allowing the creation of materials with unique microstructures. In addition, it offers significant advantages, such as being environmentally friendly, economical, and scalable (Silva, 2015).

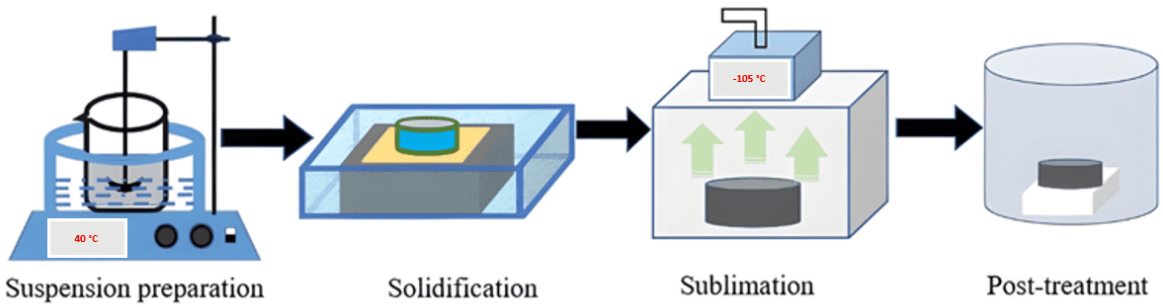

Figure 1: Schematic Diagram of the Freeze-Casting Process. (Adapted from YANG et al, 2023).

The freeze-casting process, illustrated in "Figure 1", involves several carefully controlled steps. It begins with the precise mixing of the solute and solvent. The second step, the solidification of the solvent, is particularly crucial. In this phase, the solvent is solidified under low-temperature conditions, a process that requires careful control of both the temperature and the cooling direction. This step is essential for the formation of the porous structure, as varying cooling conditions can lead to different pore sizes and shapes. Once the solvent freezes, it goes through a process called sublimation, where it transitions directly from a solid to a vapor, bypassing the liquid state. Subsequently, the formed material, still in its fragile state, goes through a sintering process, where it is heated to enhance its strength and durability. "Figure 2" illustrates different methods of controlling the cooling direction in the freeze-casting process. Each method results in a distinct pore orientation and shape in the final material, known as the "green body". For example, unidirectional freezing

results in pores aligned in the direction of the temperature gradient, while bidirectional freezing, with the introduction of a second temperature gradient, can produce pores with different alignment directions. Other methods, such as the use of a sacrificial template or the application of electromagnetic fields, can create complex and specific pore structures. Finally, for some materials such as ceramics, a high-temperature sintering process is necessary to enhance mechanical strength.

Despite advancements in the freeze-casting technique, a gap persists regarding temperature control during the process. Few works described in the literature use equipment with effective control of temperature and cooling direction. The equipment currently available predominantly use PID controllers and cooling in only one direction for monoliths (Vega, 2022; Christiansen *et al.*, 2020; Zhang *et al.*, 2018). Therefore, an opportunity was identified to innovate, using a system that allows controlled cooling for both tubes and hollow fibers, in an unprecedented way, as well as for monoliths. The equipment developed and proposed in this work is composed of a PID control and resistances and thermocouples coupled in such a way as to allow different cooling directions.

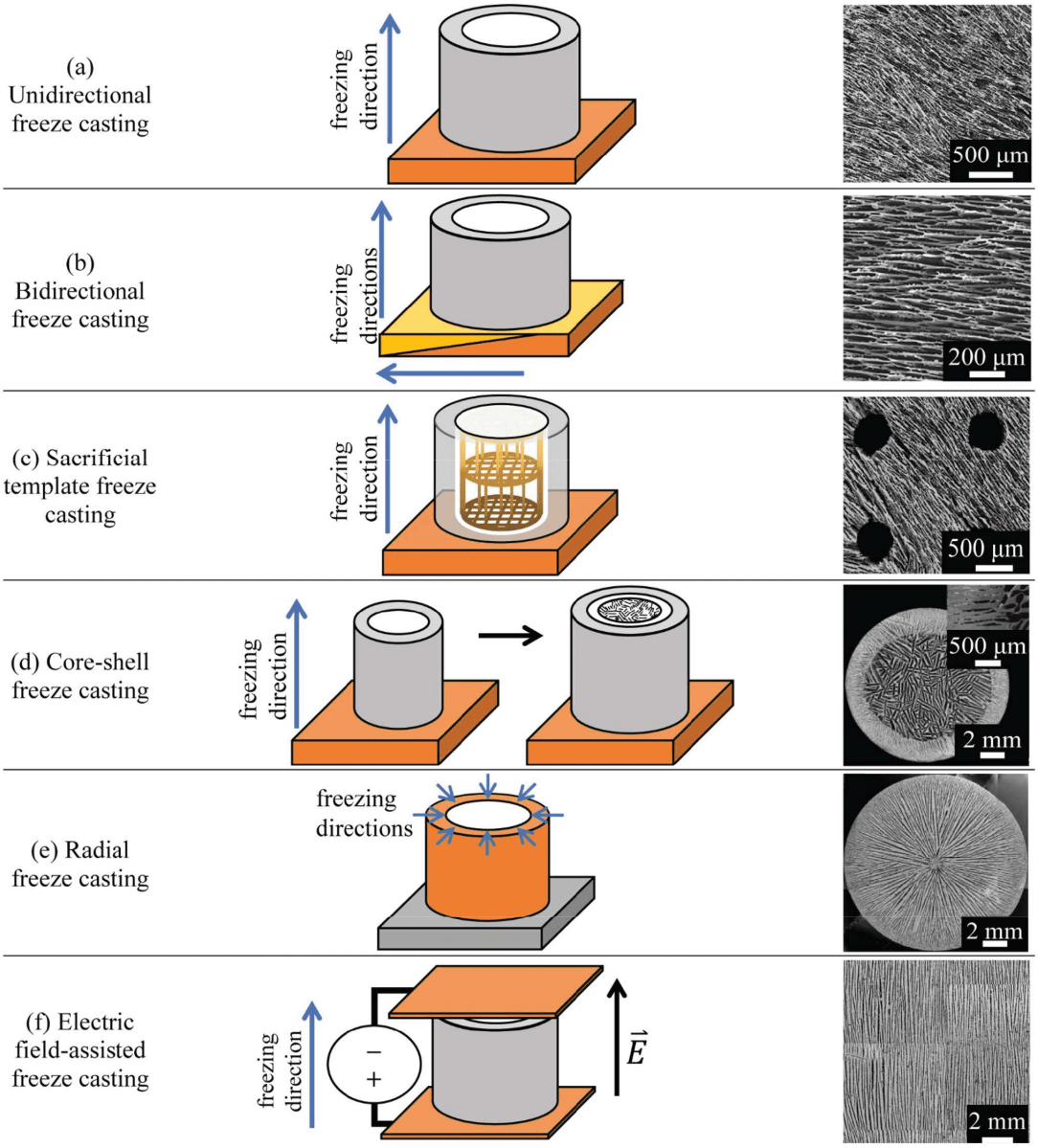

Figure 2: Freezing Directions. (Adapted from Yin and Naleway, 2022).

In the present work, was propose the development of an innovative equipment that allows the control of temperature during the freeze-casting process, in different directions using a PID control, with a maximum error of ± 1 ºC. This equipment was validated through the production of graphene oxide (GO) and chitosan (Qui) monoliths characterized by Scanning Electron Microscopy.

2. MATERIALS AND METHODS

This section describes the development of equipment aimed at the production of porous materials through the freeze-casting process. The system operates by monitoring the temperature, activating or deactivating the relays that control four electrical resistances, based on the temperature set by the user. The equipment ,“Figure 3”,is composed of a cooling unit and a control unit.

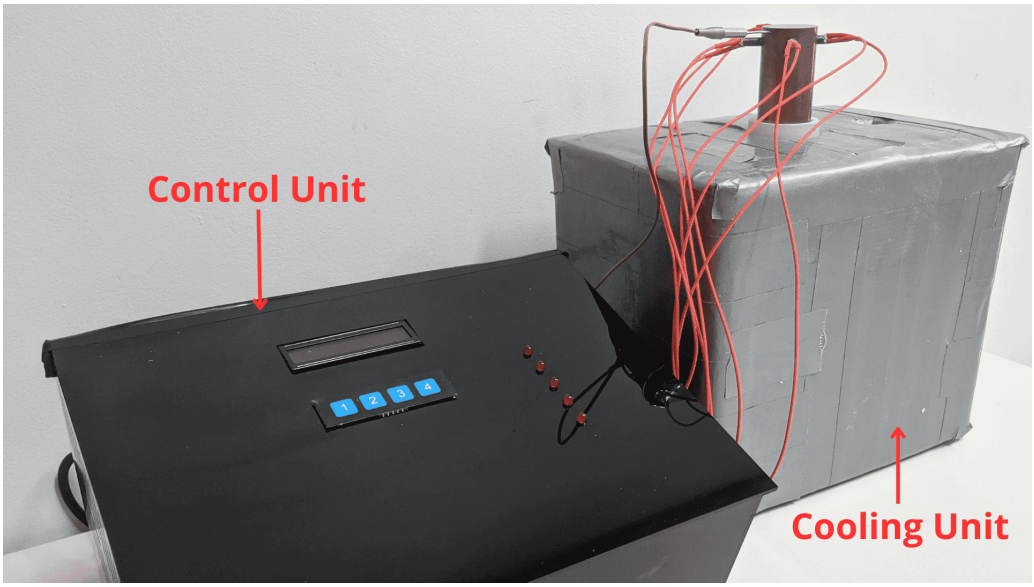

Figure 3: Control Unit and Cooling Unit.

2.1 Cooling Unit

The cooling unit, whose components are detailed in "Table 1", is composed of an insulating container with internal dimensions of 200 mm in height, 270 mm in width, and 170 mm in length, totaling a capacity of 8 liters. This container is intended for the storage of liquid nitrogen, which plays a crucial role in heat exchange with an electrolytic copper bar. The copper bar, 300 mm long and 38 mm in diameter, is inserted through the lid of the insulating container. On the upper side of the copper bar (area not submerged in $N_2(l)$), equidistant spaces of 6 mm in diameter and 15 mm in depth were drilled for the allocation of four electrical resistances. In addition, a thermocouple was inserted into a 1 mm diameter hole and 19 mm deep. The thermocouple used was of type T, and the electrical resistances, cartridge type, are similar to those used in 3D printers. Each resistance has a power of 45 W, allowing the control of the copper bar temperature in a range that varies between -196 ºC and -140 ºC, with an error margin of ± 1 ºC.

Table 1: Items that make up the cooling unit.

Material	**Quantity**
Insulating Box 8L	1
Cartridge Heater 24V 45W	4
Copper Length 300mm Diameter 38mm	1
Thermocouple	1

2.2 Control Unit

The control unit, whose materials are detailed in "Table 2", is the main point of the freeze-casting system. This unit is responsible for monitoring and adjusting the temperature during the process, ensuring that ideal conditions are maintained. The main component of the control unit is a Raspberry Pi Pico W microcontroller. This is a low-cost, high-capacity computing device that is programmed using the CircuitPython language. The developed code allows the microcontroller to monitor the current temperature and compare it with the desired temperature. Based on this comparison, the microcontroller can take measures to adjust the temperature as necessary.

To measure the temperature, the control unit uses a MAX31856 universal thermocouple amplifier. The MAX31856 amplifier reads the thermocouple voltage and converts it into a temperature reading that can be understood by the micro-

controller. Based on the temperature reading from the amplifier, the microcontroller uses a PID (Proportional-Integral-Derivative) controller to adjust the output of a PWM (Pulse Width Modulation), and can then take actions to adjust the temperature by controlling the power of the resistances. These resistances are basically heating elements that can be turned on or off to increase or decrease the temperature. The activation of these resistances is done through a DCD 2-60A type solid state relay (SSR).

Table 2: Items that make up the control unit.

Material	**Quantity**
On/Off Switch	1
Cooler	4
Display LCD with I2C	1
ESP32	1
LED	2
MAX31856	1
LM317	2
MT3608	1
Relay SSR 60A	1
Membrane Matrix Keyboard - 4 Keys	1
Triple Male Plug for Panels	1

To improve the system's power supply, an Adjustable DC-DC Voltage Booster Module (MT3608) was added between the microcontroller and the DCD 2-60 A SSR relay. The unit also includes a switched power supply for converting the voltage from 220 V to 24 V, which powers both the relay and the ESP32 and the two coolers. These last two use an LM317 voltage down module to reduce the voltage to 5 V and 12 V, respectively.

The PID controller was adjusted experimentally, modifying the Kp, Kd, and Ki coefficients and observing how the system responded in real time. Although this practical approach may seem less rigorous than analytical or model-based methods, the cited approach has the advantage of being directly applicable to complex or nonlinear systems, where mathematical models may not be accurate or easy to use. During the tuning, each coefficient was adjusted one at a time, starting with Kp, then Ki, and finally Kd. The system's response to each adjustment was closely observed, focusing on minimizing overshoot, eliminating steady-state error, and obtaining a quick and stable response. With this iterative and observational process, the PID controller was tuned to effectively and robustly control the developed equipment.

2.3 Thermal Analysis

To determine the reference temperature of the freeze-casting equipment, a series of experimental tests were conducted. In the copper rod, thermocouples were inserted into two holes: one near the upper base and another 68 mm away, corresponding to the area exposed to the environment. The test began with a 5-minute temperature reading, confirming that there is no significant difference between the upper and lower temperatures. Then, liquid nitrogen was added to the container up to 75% of its capacity to prevent overflow due to bubbling caused by heat exchange. This level of nitrogen was maintained throughout the process.

During this period, temperature readings were taken every second and a decrease in temperature was observed until stabilization. The upper temperature stabilized at -175.41 ℃ and the lower at -192.24 ℃. This process lasted approximately 15 minutes. Subsequently, the resistances were activated until the temperatures stabilized, which were -140 ℃ for the upper and -165 ℃ for the lower. The results of the experiments can be seen in "Figure. 4", which shows the temperature curve at the top (orange curve) and at the bottom (blue curve) over time.

To gain a better understanding of the temperature distribution within the cylinder, was conducted a numerical simulation under the condition of the resistance deactivated. This approach allowed us to analyze the thermal behavior more accurately. The laplacianFoam solver from the open-source software OpenFOAM 9 was employed to conduct the simulation. Using a finite volume method discretization, the solver effectively approximates the conduction equation governing the heat transfer process in a solid. The equation is expressed as:

$$\frac{\partial T}{\partial t} = \frac{\partial}{\partial x_i}\left(\alpha \frac{\partial T}{\partial x_i}\right) , \tag{1}$$

where T is the temperature, t is time, x_i represents the coordinates and α is the thermal diffusivity.

"Figure 5" shows the geometry of the cylinder and the mesh used in the simulation. Our simulation focuses solely on the external portion of the cylinder, which is in contact with the surrounding air. This external section has a length of 70 mm and a radius of 19 mm. Positioned near the top of the cylinder are four holes, for the resistances

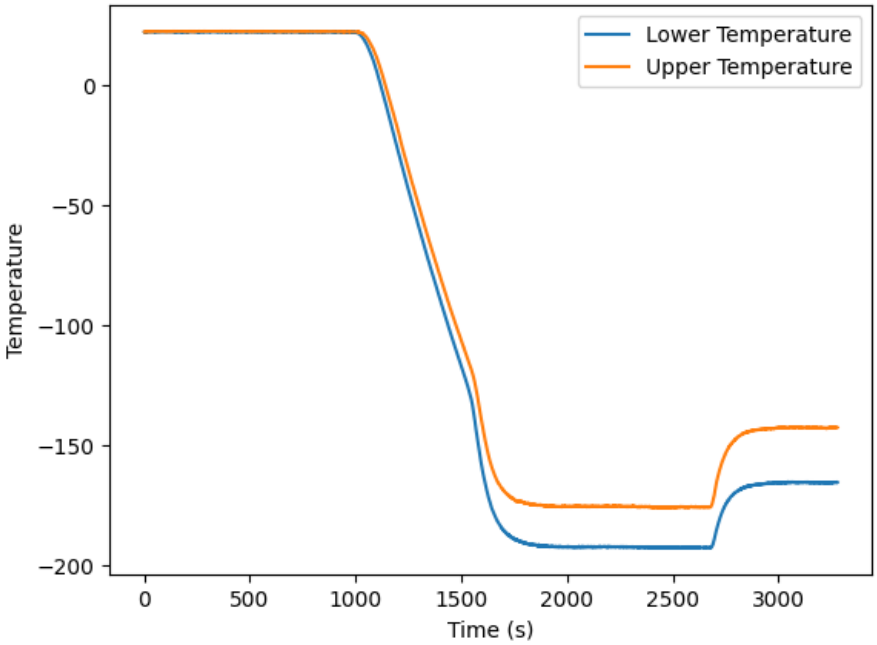

Figure 4: Upper Temperature x Lower Temperature.

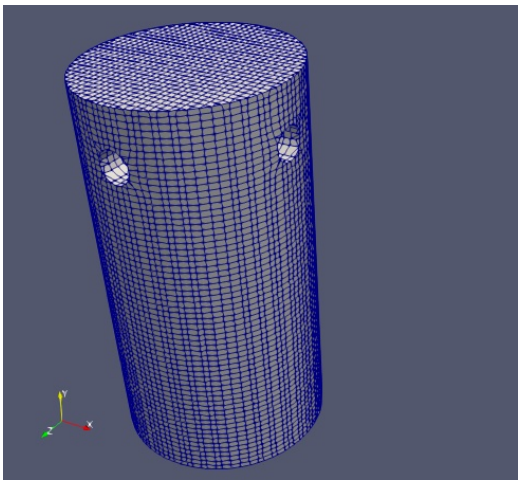

Figure 5: Geometry and mesh of the external cylinder part.

In the simulation, the experimental data is utilized as input to visualize the temperature distribution. Therefore, the temperature at the bottom plane is constant and equal to $-192\,^oC$. There is heat transfer from the surrounding air to the cylinder, through convection, which can me modeled by Newton's law of cooling,

$$\dot{Q} = hA(T_s - T_\infty) \ , \tag{2}$$

where h is the heat transfer coefficient, A is the surface area, T_s is the surface temperature and T_∞ is the external air temperature far from the cylinder surface. The convection heat transfer boundary condition is applied to the side and top surfaces of the cylinder. To obtain a temperature at the top of the cylinder of $-175\,^oC$, close to the experimental measurement, it has been adopted $h = 105\,W/(m^2 \cdot^o C)$.

The temperature distribution is shown in "Figure 6", which indicates the effect of the heat transfer from the air to the cylinder, by convection. Figure "Figure 7a" shows the temperature in the center of the cylinder, along its main axis. Another interesting result is shown in "Figure 7b", which depicts the temperature in the top plane of the cylinder. The temperature exhibits a minimum at the center, and the temperature maximum difference is $0.5\,^oC$, approximately. The top plane of the cylinder is used in direct contact with the ceramic supports during the freezing cast process and its temperature distribution influences on the quality of the material produced.

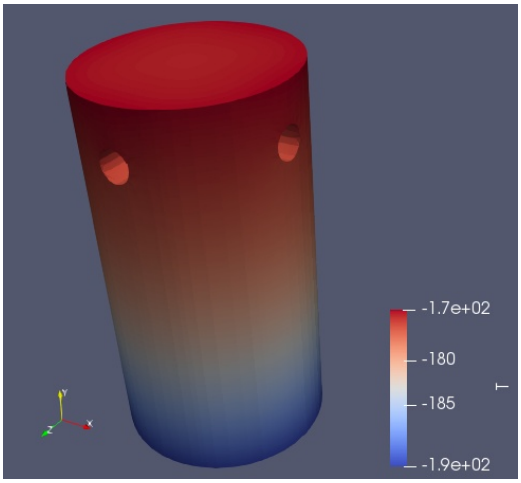

Figure 6: Temperature distribution in the cylinder. The temperature ranges from $-192\,^oC$ at the bottom to $-175\,^oC$ at the top.

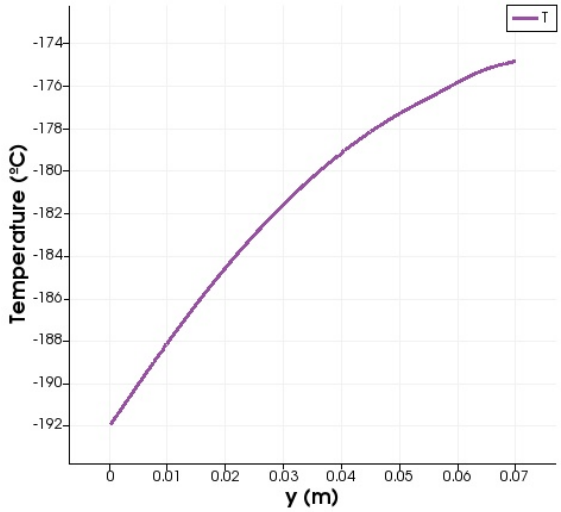

(a) Temperature along the main axis of the cylinder decreases from -192 ºC at the bottom to -175 ºC at the top.

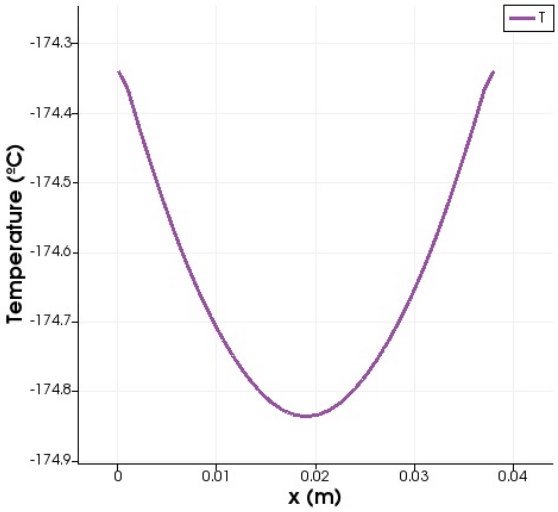

(b) Radial distribution of the temperature on the top plane of the cylinder.

Figure 7: Comparison of temperature profiles.

2.4 Preparation of Graphene Oxide (GO) and Chitosan (Qui) Monoliths

To produce the GO/Qui monoliths, a solution of 0.4673 g of chitosan in 32 mL of 4% acetic acid was prepared. This was combined with the GO suspension (5.86 g/L) in a mass ratio of Qui to GO of 8:1. The developed freeze-casting equipment was then used to control the freezing process, ensuring that the temperature remained within the desired range.

Once frozen, the monoliths underwent a process called lyophilization in the Terroni model LSE 3000 lyophilizer. Lyophilization is a drying method that involves freezing the sample and then reducing the surrounding pressure to allow the frozen ice in the material to pass directly from the solid state to the gas, a process known as sublimation. The conditions used in lyophilization were a pressure of 76 mmHg and a condenser temperature of -110 ºC. This process is delicate and preserves the porous structure created during freezing.The resulting samples were characterized using the Quanta 450 FEI scanning electron microscope with a voltage between 10 and 15kV.

2.5 Result

The validation of the equipment was carried out through the production of GO/Qui monoliths at temperatures of -170 ºC, -150 ºC, and -130 ºC, as illustrated in “Figure. 8”. The graph of freezing time as a function of temperature is shown in “Figure. 9”, indicating that the increase in solidification temperature during freeze-casting resulted in an increase in the solidification time of the GO/Qui monoliths. “Figure. 9” also presents the GO/Qui sample during freezing at -130°C."

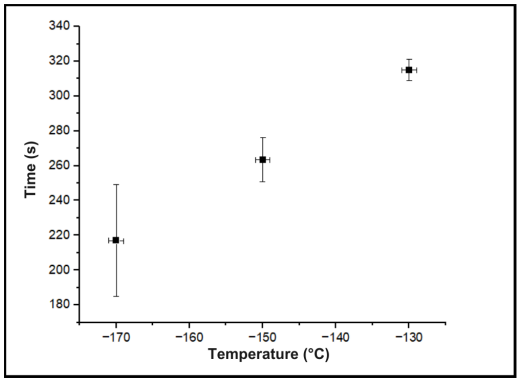

Figure 8: Temperature x Solidification time of GO/Qui.

The "Figure. 10a" presents the samples after the lyophilization process and the SEM images. The adopted methodology resulted in GO/Qui monoliths with good physical integrity. The SEM images of the GO/Qui samples in the temperatures of -130 ºC, -150 ºC, and -170 ºC show that in the lower the temperature, smaller is the distance between the GO walls, as the ice crystals that originate the pores are smaller. Therefore, the developed freeze-casting equipment allows the manufacture of materials with different pore sizes through precise control of the freezing temperature and based on solidification theory.

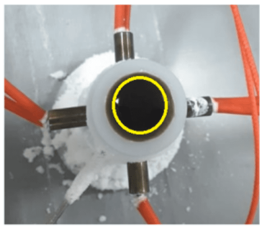

(a) Start of surface solidification ≈ 280 s.

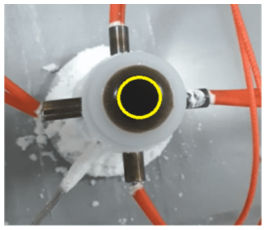

(b) Intermediate stage ≈ 290 s.

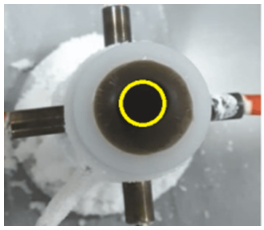

(c) Intermediate stage ≈ 300 s.

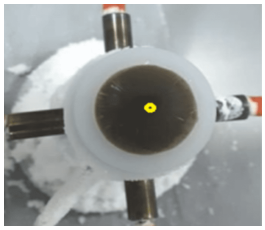

(d) Complete solidification ≈ 310 s.

Figure 9: GO/Qui sample during freezing at -130 ºC to different time of solidification: (a) 280 s, (b) 290 s, (c) 300 s, (d) 310 s.

3. CONCLUSIONS

In this study, It has been highlighted a significant advancement in the production of porous materials through the development of a microcontrolled equipment that enhances temperature control during the freezing stage in the freeze-casting process. The precision of ±1ºC, obtained through PID control, sets a milestone in the production of ceramic bodies with an aligned structure and varied levels of porosity. This precision opens up a range of possibilities for the customization of materials, increasing their versatility and applicability in various areas.

The precision of temperature control, coupled with the robustness and flexibility of the implemented system, allows the equipment to be easily adapted to meet new needs or requirements. This could include the addition of new features or the adaptation of the equipment to work with different freezing directions. The characterization of graphene oxide (GO) and chitosan (Qui) monoliths through Scanning Electron Microscopy (SEM) revealed the existence of distinct structures corresponding to temperatures of -130 ºC, -150 ºC, and -170 ºC. This evidences the effectiveness of the equipment, allowing the application of the generated material in various areas of the industry.

The efficiency of the equipment, coupled with low error and cost, establishes it as a viable and economical solution for the production of porous materials. Therefore, this work represents a milestone in the materials field, offering an efficient, innovative, and safe solution for temperature control during the freeze-casting process. It is expected that this advancement will drive new research and applications, significantly contributing to the progress of the study of materials produced through freeze-casting.

4. ACKNOWLEDGEMENTS

The authors would like to acknowledge the company Petronas, Foundation for Research Support of the Federal District (FAP-DF) and the Foundation for Scientific and Technological Enterprises of Brazil (FINATEC) for the support given to

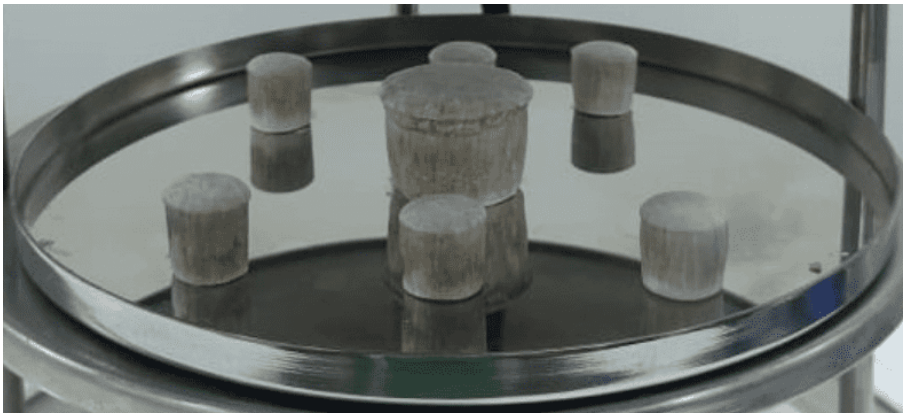

(a) GO/Qui samples after lyophilization.

(b) -170 ºC

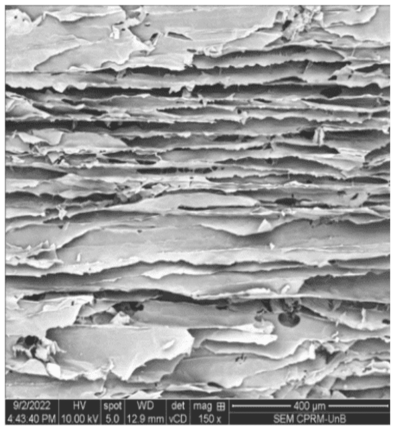

(c) -150 ºC

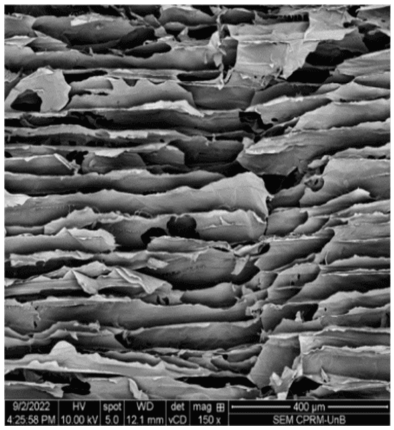

(d) -130 ºC

Figure 10: "Figure. 10a" samples after lyophilization. Horizontal view x150 applies to Figures " 10b", " 10c", and " 10d". It is evident that lower temperatures result in smaller pore sizes. Specifically, at -170ºC "Figure. 10b", the interlamellar spacing is virtually undetectable. On the other hand, at -150ºC "Figure. 10c", the interlamellar spacing is more evident than at -170ºC. At -130ºC "Figure. 10d", the interlamellar spacing is greater than what is observed at both -150ºC and -170ºC.

carry out this work; for the support of the Microscopy Laboratory of the Institute of Geosciences and the Laboratory of Microscopy and Microanalysis of UnB, the Center for the Development of Nuclear Technology and the Microscopy Center at UFMG.

5. REFERENCES

Christiansen, C.D., Nielsen, K.K. and Bjørk, R., 2020. "Novel freeze-casting device with high precision thermoelectric temperature control for dynamic freezing conditions". *Review of Scientific Instruments*, Vol. 91, No. 3, p. 033904. ISSN 0034-6748, 1089-7623. doi:10.1063/1.5134737. URL https://pubs.aip.org/aip/rsi/article/1031784.

Scotti, K.L. and Dunand, D.C., 2018. "Freeze casting – A review of processing, microstructure and properties via the open data repository, FreezeCasting.net". *Progress in Materials Science*, Vol. 94, pp. 243–305. ISSN 00796425. doi:10.1016/j.pmatsci.2018.01.001. URL https://linkinghub.elsevier.com/retrieve/pii/S007964251830001X.

Silva, A.M.A., 2015. *Obtenção e Caracterização de Cerâmicas Porosas pelo Processo de Freeze Casting*. Ph.D. thesis, Universidade Federal de Minas Gerais. URL https://ppgem.eng.ufmg.br/defesas/2110D.PDF?src=10872.

Sousa, B.M., Athayde, D.D. and Vasconcelos, W.L., 2021. "Mechanical Behavior of Tubular Freeze-Cast Substrates with Organized Pore Structure". *Materials Research*, Vol. 24, No. 5, p. e20210127. ISSN 1980-5373, 1516-1439. doi:10.1590/1980-5373-mr-2021-0127. URL http://www.scielo.br/scielo.php?script=sci$_arttextpid = S1516 - 14392021000500217tlng = en.$

Souza, D.F., Nunes, E.H., Pimenta, D.S., Vasconcelos, D.C., Nascimento, J.F., Grava, W., Houmard, M. and Vasconcelos, W.L., 2014. "Synthesis and structural evaluation of freeze-cast porous alumina". *Materi-*

als Characterization, Vol. 96, pp. 183–195. ISSN 10445803. doi:10.1016/j.matchar.2014.08.009. URL https://linkinghub.elsevier.com/retrieve/pii/S1044580314002502.

Vega, S.A.R., 2022. *Diseño y construcción de un aparato de Freeze-Casting para la fabricación de probetas cerámicas con porosidad alineada*. Ph.D. thesis.

Yin, T.J. and Naleway, S.E., 2022. "Freeze Casting with Bioceramics for Bone Graft Substitutes". *Biomedical Materials & Devices*. ISSN 2731-4812, 2731-4820. doi:10.1007/s44174-022-00008-1. URL https://link.springer.com/10.1007/s44174-022-00008-1.

Zhang, H., Liu, S., Xiao, H. and Zhang, X., 2018. "Synthesis and Tribological Properties of Bio-Inspired Nacre-Like Composites". *Materials*, Vol. 11, p. 1563. doi:10.3390/ma11091563.

6. RESPONSIBILITY NOTICE

The authors are solely responsible for the printed material included in this paper.